Extragalactic jets from every angle
Proceedings IAU Symposium No. 313, 2014
F. Massaro, C. C. Cheung, E. Lopez, A. Siemiginowska, eds.

doi:10.1017/S1743921315002069

Polarimetric tomography of blazar jets

Ulisses Barres de Almeida,[1] Fabrizio Tavecchio[2] and Nijil Mankuzhiyil[3]

[1]Centro Brasileiro de Pesquisas Físicas
Rua Dr. Xavier Sigaud 150, RJ – 22290-180, Rio de Janeiro, Brazil
email: ulisses@cbpf.br

[2]Osservatorio Astronomico di Brera, Via Emilio Bianchi 46, 23807 Merate, Italy
email: fabrizio.tavecchio@brera.inaf.it

[3]Astrophysics Science Division, BARC, 400085 Mumbai, India
email:mankuzhiyil.nijil@gmail.com

Abstract. In this talk we present a novel way to use optical polarimetric observations to provide independent constraints and guide to the modelling of the spectral energy distribution (SED) of blazars. The approach is particularly useful to judge when a two-zone model description of the SED of the source is required and is able to provide with extra information that helps breaking some of the degeneracies on the fit parameters of the two SSC model components. The method will be presented in some detail and will be subsequently applied to the 2008 multi-wavelength campaign of PKS 2155-304 as an illustration of its potential.

Keywords. polarization, techniques: polarimetric, galaxies: active

1. Introduction

Active galactic nuclei (AGN) have a strongly non-isotropic radiative output, with a pair of relativistic jets emanating at opposite directions from the central engine. When the observer's line-of-sight happens to be aligned with the outflow direction, the object is called a blazar (Urry & Padovani 1995). The radiation Doppler boost resulting from this chance alignment renders blazars the dominant extragalactic source class in the sky above 100 GeV (Hinton & Hofmann 2009).

Modelling of the broadband spectral energy distribution (SED) is a well established technique to study the physics of blazars (Ghisellini *et al.* 1998). The general double-hump structure of the SED is well explained as synchrotron and inverse-Compton radiation from a highly energetic population of electrons. Evidence from MWL observations shows that the AGN emission is variable at all frequencies, and contemporaneous measurements indicate the SED to be remarkably correlated (Fossati *et al.* 1998).

Although one-zone models (e.g., Maraschi *et al.* 1992, Sikora *et al.* 1994, Bloom & Marscher 1996) have been successful in describing the SED of blazars, recent MWL observations have revealed the necessity of adopting multi-zone models at least in some cases (e.g., Aleksic *et al.* 2012, Abramowski *et al.* 2012).

Given the degeneracy and large number of parameters present in these inhomogenous SED models – at least 12 for a two-zone SSC – some independent insight into the properties of the different particle populations that are simultaneously contributing to the observed emission would be decisive to better motivate and provide additional constraints to models. Our proposal in this work aims to do exactly this. For more details on this work see Barres de Almeida *et al.* (2014).

2. Optical polarisation in blazars

The polarised emission from blazars was discovered early on in the observations of these objects in the 60's, and was readily interpreted as the signature of synchrotron radiation from a non-thermal distribution of relativistic particles – for a review of early developments in the field see Angel & Stockman (1980). Since then it has been an important technique to study the physics of blazar jets.

In radio, milli-arcsecond resolution polarisation interferometry allows for a mapping of the magnetic field state along the jet and the possibility to physically locate its active emission regions (D'Arcangelo *et al.* 2009, Agudo *et al.* 2011).

Even if the inner jets of blazars cannot be resolved in optical waveband, polarisation observations at these frequencies are an avenue to probe their internal structure. Turbulence is long believed to dominate plasma flow at small scales (Moore *et al.* 1982). Plasma turbulence reflects in the state of the magnetic field, resulting in a tangled structure which reduces the mean source polarisation to few percent and imprints randomness to the source behaviour, except when some mechanism is at play (if only temporarily) that imparts order to the field, either locally (e.g., by shock compression; see Laing 1980) or globally (e.g., a toroidal or helical B-field configuration; see Lovelace *et al.* 2002). When internal shocks enhance the emissivity of a portion of the jet, the polarisation of this active zone can dominate that of the entire source, adding coherence to it.

3. Polarimetric tomography

We will present an original approach to the modelling of blazar SEDs which directly incorporates information provided by optical polarimetric observations in the models to provide additional constraints and guide the fits with independently-motivated physical inputs. The motivation for this work basically stems from the question: *"Can we do more with the optical polarimetric observations to the study of blazars than currently achieved?"* What we verified is that through the approach proposed here we can look "inside the unresolved optical jet" and single out the dominant active regions responsible for the variability of the source, thus finding a way to disentangle the multi-zone SEDs.

The optical polarimetric analysis at the basis of the technique has been originally proposed by Hagen-Thorn & Marchenko (1999) and re-applied by Barres de Almeida *et al.* (2010) (henceforth BA10). The power of the analysis resides in the fact that it allows to identify the single component which contributes the most to the source activity, separating it from the rest of the "quiescent jet".

In fact, since the degree of polarisation can be quite high (relative to the source's average) in the most active emission sites of the jets – think of the VLBI images of the jets where the high-emissivity jet knots present an enhanced degree of polarisation – these singular zones can dominate the source emission when seen in polarised light, even when their photometric output is far less than that from the rest of the "quiescent" jet. In addition to that, these are also the regions which tend to be responsible for the bulk of the source variability, especially at higher energies, where we know, from detection of fast-variability episodes, that the most active zones are likely to be specific areas within the jet.

This means that observing the source in polarised light can potentially serve as a "tomography" probe into its different emission zones, and its internal structure can be revealed even when the object is unresolved via direct imaging. For our specific concerns – i.e., to independently justify and constrain a specific SED model for blazars – this is equivalent to deciding if a one-or two-zone model must be adopted to explain the

https://doi.org/10.1017/S1743921315002069 Published online by Cambridge University Press

polarisation behaviour in the optical band. And then, since one expects the variable polarised region to be active at higher frequencies as well via synchrotron self-Compton emission, characterising it at these low frequencies has an impact in the entire SED fit.

The details of the polarisation analysis are discussed in BA10 and in Barres de Almeida *et al.* (2014), but in summary what one does is to analyse the variability of the Stokes parameters of the source, and evaluate if this variability can be described by the evolution of a single zone or if the superposition of two variable components is necessary to explain the main features of its evolution. For example, if the temporal changes in Q and U are related in a linear fashion with the total flux variability I, as described in Hagen-Thorn & Marchenko (1999), then this suggests that the source variability is motivated by a region with constant polarisation properties within a given timescale. Through the linear regression analysis one can then distinguish the properties of this specific zone to those of the rest of the jet, providing the physical constraints which will serve as input to the inhomogeneous SED model, as exemplified in the next section.

4. Application to PKS 2155-304

In September 2008, the VHE blazar PKS 2155-304 was jointly observed by H.E.S.S. and Fermi in an extensive MWL campaign, accompanied also by X-ray, optical, and optical polarimetric data (Aharonian *et al.* (2009) and BA10).The source was found to be in a low state throughout the period and constant in gamma-rays, with the optical flux showing only modest flickering. The X-ray flux has in the other hand shown significant variations which could not be clearly correlated to the bahaviour seen in any of the other bands. Aharonian *et al.* (2009) interpreted the source emission as a single-zone synchrotron self-Compton (SSC) model, but noted that the one-region scheme could not explain both the SED and its variability.

It was nevertheless observed that the polarisation of the source was variable. A detailed analysis of the data by BA10 showed that the polarisation behaviour could be interpreted as the interplay between two zones: a variable component and the steady jet. In this scenario, the photometric flux changes would be completely hidden by the larger flux of the broader jet, the active region being responsible for only $\sim 10\%$ of the total flux.

When the behaviour of the variable zone is compared with the previously unexplained X-ray variability, a matching trend is seen between the two (Fig. 1), suggesting the X-ray variability could be due to variations of this active portion within the steady-emission jet. The previously unidentified optical properties of the component, probed thanks to the polarisation analysis, gives us the missing constraint for performing a self-consistent fit of the entire SED, interpreted as an independently-motivated two-zone model.

5. The SED modelling

To reproduce the SED of each component we adopted a standard leptonic model (Tavecchio *et al.* 1998). The emission region is described as a sphere of radius R, filled with magnetic field of intensity B and relativistic electrons following a smooth broken power law energy distribution, between Lorentz factors $\gamma_{\rm min}$ and $\gamma_{\rm max}$, with slopes n_1, n_2 below and above the break $\gamma_{\rm b}$. Relativistic effects on the observed radiation are fully described by the Doppler factor δ.

The optical polarisation analysis described suggests that, at least in optical, the data set is well described by a two-zone model, composed of a steady component, and a variable one, responsible for the variability seen in polarised light, but only for 10% of the total photometric flux. The observed correlation found in Fig. 1 between the X-ray variability

https://doi.org/10.1017/S1743921315002069 Published online by Cambridge University Press

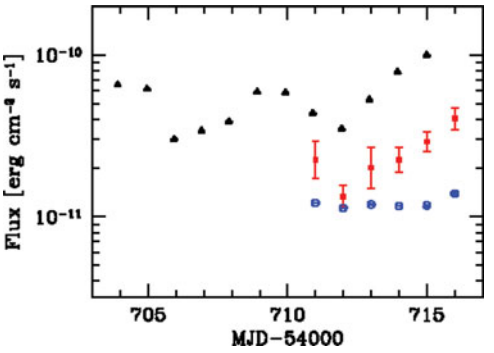

Figure 1. Contemporaneous light curves for PKS 2155-304 from September 2008. Black triangles show the RXTE (2-10 keV) light-curve. Squares represent the optical flux behaviour of the variable component as derived from the polarimetric analysis. Note the matching trend between the source's total X-ray flux and the variability of the compact component. The open circles which refer to the total optical flux light curve for the source (scaled down by a factor of 0.1 to fit the image scale) that does not show the same clear correlation with the X-ray data.

and the optical flux of the variable component suggests that the X-ray changes are driven exclusively by the behaviour of this portion of the jet, thus providing a tight physical constraint to the two-zone model SED fit.

In principle, these two regions could be spatially distinct or, alternatively, the system could be composed by a compact zone embedded into a larger jet. For simplicity, we do not consider this scenario here, because it would involve the complex treatment of the radiative interplay between the two zones. We treat each component as independent and assume that within each region the inverse-Compton emission derives only from the scattering of the locally produced synchrotron photons. From the point of view of the emission model this assumption is enough to fully specify the system. From the physical point of view, if the two regions have comparable bulk Lorentz factor and comparable synchrotron luminosities (as is the case), there is no relative beaming of the two radiation fields. Therefore, to ensure the radiative independence of the two components it is enough that the distance separating the two regions is a few times their radii.

To proceed with the fit we first fix the steady component, constrained by the steady optical flux and the LAT and H.E.S.S. spectra. A further constraint to this component derives from the condition that its contribution to the X-ray emission must be very low in order to preserve the correlation shown in Fig. 1. These conditions are stringent enough to provide tight constraints to the spectral shape and the model parameters for the steady component. In practice, we assumed that the flux at the Fermi peak spectrum position and $\sim 90\%$ of the peak optical flux (as derived from polarimetric analysis) are coming from the steady component alone, equal at each night, allowing for only 10% variability which is permitted by the data. Then, fixing $\gamma_{\rm min} = 1000$, a χ^2 fit of the steady SED was produced following Mankuzhiyil *et al.* (2012). The values are shown in Table 5.

Once the steady SED is fixed, we started to reproduce the variable emission, restricted by the daily optical and X-ray measurements. To fit the variable component of the SED and derive the SSC model parameters we followed the same χ^2 minimisation procedure, in which the minimum of the χ^2 is calculated using the sum of the variable and the quiescent component. Here we assumed that the size of the emission region remained constant throughout the period, hence fixing the radius of the variable blob as $R = 1.5 \times 10^{16}$ cm, which is a typical value adopted in the literature. The radius of the constant component instead was produced as a result of the numerical fit, by assuming the optical and Fermi

https://doi.org/10.1017/S1743921315002069 Published online by Cambridge University Press

Table 1. Input model parameters to the daily SED fits.

State	γ_{min} [10^3]	γ_b [10^5]	γ_{max} [10^6]	n_1	n_2	B [10^{-2} G]	K [10^3 cm^{-3}]	R [10^{16} cm]	δ
Steady	1.0	0.4	0.1	2.0	4.5	10.0	1.0	2.0	35.0
MJD 54711	1.0	$1.11^{0.03}_{0.03}$	$30.1^{7.7}_{0.5}$	$2.109^{0.004}_{0.004}$	$4.82^{0.06}_{0.06}$	$7.6^{0.1}_{0.2}$	$5.8^{0.3}_{0.2}$	1.5	$27.90^{0.03}_{0.03}$
MJD 54712	1.0	$1.35^{0.04}_{0.03}$	$30.3^{1.0}_{0.4}$	$2.097^{0.004}_{0.004}$	$4.61^{0.06}_{0.07}$	$6.9^{0.2}_{0.1}$	$8.1^{0.4}_{0.3}$	1.5	$22.12^{0.03}_{0.05}$
MJD 54713	1.0	$1.03^{0.04}_{0.03}$	$31.0^{1.0}_{0.4}$	$2.139^{0.003}_{0.004}$	$4.11^{0.05}_{0.05}$	$6.6^{0.2}_{0.1}$	$8.3^{0.4}_{0.3}$	1.5	$28.05^{0.03}_{0.03}$
MJD 54714	1.0	$1.14^{0.04}_{0.03}$	$72.2^{5.2}_{48.0}$	$2.147^{0.004}_{0.004}$	$4.20^{0.06}_{0.06}$	$8.4^{0.2}_{0.2}$	$7.2^{0.3}_{0.3}$	1.5	$27.76^{0.03}_{0.01}$
MJD 54715	1.0	$0.76^{0.03}_{0.03}$	$25.2^{3.6}_{0.3}$	$2.139^{0.004}_{0.004}$	$3.77^{0.04}_{0.04}$	$10.02^{0.02}_{0.02}$	$6.7^{0.3}_{0.3}$	1.5	$27.78^{0.03}_{0.02}$

Notes: For each state we report: minimum, break and maximum Lorentz factors of the electron distribution, low and high energy slope, magnetic field, electron density, radius of emitting region and its Doppler factor.

peaks being dominated by it. Due to the lack of high-frequency radio interferometric observations during the period, it is difficult to constrain γ_{min}. We have therefore opted to fix $\gamma_{min} = 1000$, but other cases have been checked and we found that our assumption does not significantly impact on the determination of the other parameters. Finally, we kept all the other 7 parameters free to float in the minimization procedure, to avoid biases to the final solution.

The resulting fit parameters are shown in Table 5. They validate a scenario (Fig. 2) where the difference in the daily flux states result from changes in B, and are accompanied by some evidence of contemporaneous changes in the electron density, K. Along with these, changes were registered in the high-energy spectral slope n_2, which shows a fairly steady decrease during the campaign, and we found as well some evidence for possible changes in the break Lorentz factor γ_b.

6. Conclusions

We have presented a new approach to the modelling of the blazar SEDs which uses an analysis of the optical polarisation state of the source to provide additional motivation and constraints to advance a multi-zone SED model for the source. Such information is then used to parameterise, in a highly constrained fashion, the inhomogeneous SED model. In the example shown here we were able to derive a two-component model for PKS 2155-304 which described its spectral distribution and temporal evolution in good detail, allowing for a simple physical description of the results, in a self-consistent way.

The fact that the polarisation analysis can disentangle the behaviour of a sub-component of the jet whose flux might be only a small fraction of the total emission is the key strength of the technique. The case presented here in fact suggests that this kind of analysis might bear relevance to understanding MWL correlations and orphan flares in blazars. Of particular relevance as well is the fact that our result suggests a two-component model for a low activity state of the source. It is still to be verified what the technique would say about high-states, where a single dominant zone might be enough to describe the source's SED. This project is currently being complemented by a larger set of new optical polarimetric observations of TeV blazars and we expect to publish the new results soon.

https://doi.org/10.1017/S1743921315002069 Published online by Cambridge University Press

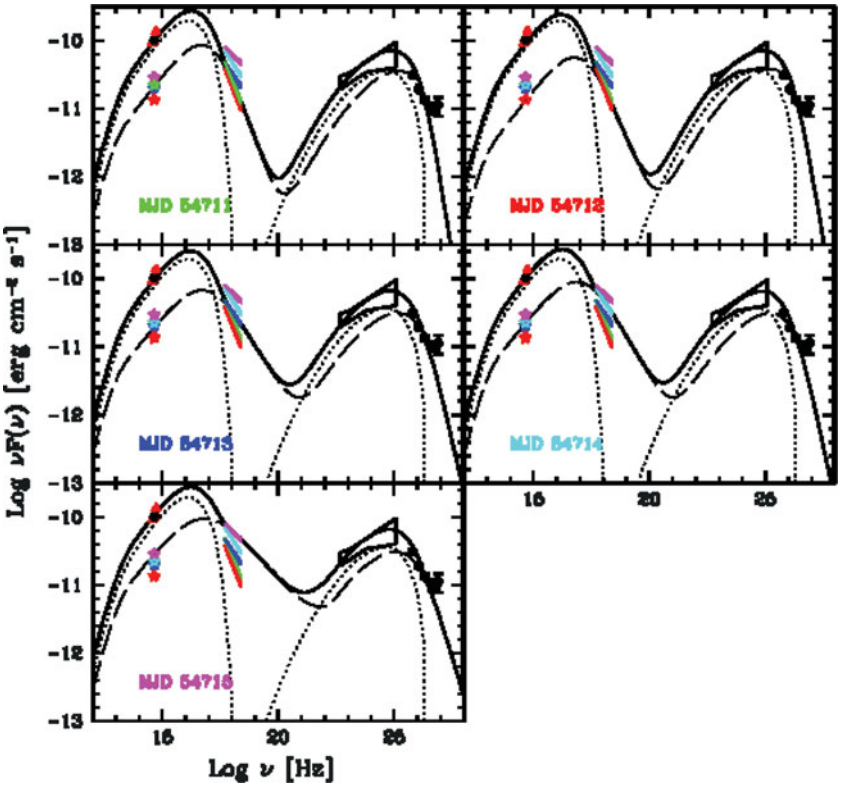

Figure 2. Nightly fits for the SED of PKS 2155-304. The dasehd line represents the SED model of the variable region, responsible for the correlated optical and X-ray changes. Dotted lines represent the SED of the steady jet, main contributor to the non-variable gamma-ray flux. The total SED is shown with the thick black line as the sum of the two components.

References

Abramowski, A., *et al.* (H. E. S.. S. Collaboration) 2012, *A&A*, 539, 149
Agudo, I, Marscher, A. P., Jorstad, S., *et al.* 2011, *ApJL*, 735, L10
Aleksic, J., *et al.* (MAGIC Collaboration) 2012, *A&A*, 542, 100
Angel, J. R. P.. & Stockman, H. S. 1980, *ARA&A*, 18, 321
Barres de Almeida, U., Ward, M. J., Dominici, T. P., *et al.* 2010, *MNRAS*, 408, 1778
Barres de Almeida, U., Tavecchio, F., & Mankuzhiyil, N. 2014, *ApJ*, 441, 2885
Bloom, S. D. & Marscher, A. P. 1996, *ApJ*, 461, 657
D'Arcangelo, F. D., Marscher, A. P., Jorstad, S. G., *et al.* 2009, *ApJ*, 697, 985
Fossati, G., Maraschi, L., Celotti, A., *et al.* 1998, *MNRAS*, 299, 433
Ghisellini, G., Celotti, A., Fossati, G., *et al.* 1998, *MNRAS*, 301, 451
Hagen-Thorn, V. A. & Marchenko, S. G. 1999, *BaltA*, 8, 575
Hinton, J. & Hofmann, W. 2009, *ARA&A*, 47, 523
Laing, R. A. 1980, *MNRAS*, 193, 439
Lovelace, R., Li, H., Koldoba, A. V., *et al.* 2002, *ApJ*, 572, 445
Mankuzhiyil, N., Ansoldi, S., Persic, M., *et al.* 2012, *ApJ*, 753, 154
Maraschi, L., Ghisellini, G., & Celotti, A. 1992, *ApJL*, 397, 5
Moore, R. L., Angel, J. R. P., Duerr, R., *et al.* 1982, *ApJ*, 260, 415
Sikora, M., Begelman, M., & Rees, M. 1994, *ApJ*, 421, 153
Tavecchio, F., Maraschi, L., & Ghisellini, G. 1998, *ApJ*, 509, 608
Urry, C. M. & Padovani, P. 1995, *PASP*, 31, 473

https://doi.org/10.1017/S1743921315002069 Published online by Cambridge University Press